Power and Mean Flow Characteristics in Mixing Vessels Agitated by Hyperboloid Stirrers

F. T. PINHO[a)*], *F. M. PIQUEIRO*[b)], *M. F. PROENÇA*[b)] *and A. M. SANTOS*[c)]

[a)]*Departamento de Engenharia Mecânica e Gestão Industrial, Faculdade de Engenharia, Rua dos Bragas, 4099 Porto Codex, Portugal*

[b)]*Departamento de Engenharia Civil, Faculdade de Engenharia, Rua dos Bragas, 4099 Porto Codex, Portugal*

[c)]*Instituto de Engenharia Mecânica e Gestão Industrial, Unidade de Térmica Industrial, Rua do Barroco 174, 4465 S. Mamede de Infesta, Portugal*

The mean flow and energy consumption in vessels powered by hyperboloid stirrers was investigated. The Newton number followed an inverse linear law for Reynolds numbers below approximately 200, which had values more than twice higher the corresponding Newton number for a standard Rushton turbine. At high Reynolds number flows the Power number varied between 0.5 for a $D/T = 0.78$ impeller to 0.95 for a $D/T = 0.24$ impeller, as compared to a value of 5 for the standard Rushton stirrer, and to values of 0.31 and 1.58 for the Chemineer and Prochem hydrofoils. The power consumption did not change with the fluid height and was double for the double-stack configuration. The shear ribs below the impeller were the main contributor to the increased energy loss relative to a non-shear ribbed impeller and the small clearance had no major effect upon the power consumption. For the $D/T = 1/3$ hyperboloid stirrer the flow in the whole tank was rather gentle, defining a circulation number of 0.57, thus leading to a circulation efficiency more than 7 times lower than that of the hydrofoils.

On a étudié l'écoulement moyen et la consommation d'énergie dans des réservoirs agités par des turbines hyperboloïdes. Le nombre de Newton suit une loi inversement proportionnelle au nombre de Reynolds au-dessous d'environ 200, ce qui est plus de deux fois supérieures à ce qui est obtenu avec une turbine de Rushton standard. Pour des écoulements à nombre de Reynolds élevé, le nombre de puissance varie entre 0,5 pour une turbine de $D/T = 0,78$ et 0,95 pour une turbine de $D/T = 0,24$, comparativement à une valeur de 5 pour l'agitateur Rushton standard, et à des valeurs de 0,31 et 1,58 pour les turbines profilées de chez Chemineer et Prochem. La consommation d'énergie ne change pas avec la hauteur du fluide et est doublée pour la configuration à double turbine. Les ailettes de cisaillement sous la turbine sont le principal facteur contribuant à une plus grande perte d'énergie par rapport à une turbine sans ailettes de cisaillement, et le petit dégagement n'a aucun effet majeur sur la consommation d'énergie. Pour l'agitateur hyperboloïde de $D/T = 1/3$, l'écoulement dans l'ensemble du réservoir est plutôt modéré, donnant un nombre de circulation de 0,57, ce qui conduit à une efficacité de circulation de plus de 7 fois inférieure à celle des turbines profilées.

Keywords: stirred tank, hyperboloid impeller, power consumption.

Mixing vessels are commonly encountered in many engineering applications within the domain of chemical engineering, as well as in hydraulics, for instance in waste water treatment plants. A proper design and optimization of mixing systems requires a detailed knowledge of the flow hydrodynamics, conditions of operation of the reactor and its relation with the various relevant geometrical parameters, such as tank geometry, impeller type and size and number of impellers (Oldshue, 1983, Ulbrecht and Patterson, 1985), as well as type of process and the nature of the fluids (Skelland, 1983).

Mechanically agitated mixed flows have been investigated for quite a long time for a large variety of process applications, agitators, fluids, as well as flow and geometrical parameters (Nagata, 1975, Skelland, 1967). The most investigated flow case is undoubtedly that of the vessel agitated by the Rushton impeller, now used as a standard for comparison purposes and to help develop and validate design codes, although the industry has opted in many instances for more efficient stirrers (Joosten et al., 1977), as is the case of hydrofoils.

The detailed Laser-Doppler velocity measurements of Reed et al. (1977) and Popiolek et al. (1987) have shown the formation of two wall jets from the impingement at the vessel wall of the radial jet coming out of the impeller plane of a Rushton stirrer, as well as the flow separation behind the impeller blades. With their angle-resolved measurements the latter workers concluded that the turbulent kinetic energy in the radial jet was 10 times higher that in the remaining of the vessel. These measurements were further extended to include solids suspensions by Nouri and Whitelaw (1992) and non-Newtonian fluids by Hockey (1990), who performed an energy balance around the stirrer. More recently, Rutherford et al. (1996 a,b) concentrated on assessing the impeller blade thickness effect and the main flow characteristics of the double stack configuration, respectively. The interaction between turbulence and the kinetics of aggregates has also been thoroughly investigated by Kusters (1991).

More efficient agitation systems have been developed and investigated over the years for different purposes: Buckland et al. (1988) and Bakker and van den Akker (1990) have shown that axial hydrofoil impellers are better for gas dispersion than conventional agitators. Recently, Höfken et al. (1991) designed the new hyperboloid impeller from considerations of Fluid Dynamics aimed at ensuring a complete suspension of particles and a good dispersion of air bubbles, without destroying the suspended microorganisms, in view of its applications to sludge treatment.

*Author to whom correspondence should be addressed.

Nouri and Whitelaw (1994) have shown that the hyperboloid stirrer was better than the Rushton impeller in terms of power consumption and investigated the effects of impeller clearance and diameter upon the flow characteristics. Their hyperboloid impeller had transport ribs at the upper surface and they concluded that smaller off-bottom clearances, of the order of 1/10, improved the particle suspension performance, as measured by the Zwietering parameter. Although this parameter was not as good as for Rushton agitated vessels, the energy requirements were 20 times lower.

The aeration studies of Höfken et al. (1991) led to an improved design of the hyperboloid impeller with the incorporation of shear ribs at the edge of the bottom surface of the agitator for breaking up gas bubbles more efficiently. The efficient aeration from below the impeller also required it to be located close to the bottom of the vessel so that the whole flow could be aerated. However, there is a lack of information on the hydrodynamic behaviour of the flow powered by this impeller under such configuration and this work is intended as a contribution to such knowledge.

The characterization of this mixing vessel flow will be carried out in three stages: initially, an investigation of the global flow properties, such as the relationship between rotational speed and power input for various impeller sizes and number of agitators, together with flow visualization and measurements of the mean flow field, will provide a fairly good picture of the main parameters controlling the flow. Later on, more detailed measurements of the velocity field will provide data for assessing some micromixing characteristics, for performing an energy balance around the impeller, and for investigating the extent of the flow periodicity created by the ribs. Finally, process measurements as well as the investigation of aerated flows will be required.

This paper addresses the first part of the work and compares the results with similar data pertaining to stirred vessels powered by standard Rushton, pitched blade and less conventional impellers, so that a measure of the advantages/disadvantages of this new system are properly documented and put into perspective. In the next section, the experimental facility and the measuring procedures and uncertainties are described. Then, the power measurement results are presented and discussed for various flow configurations, and one of them is selected for mean flow field mapping and further calculations of overall parameters. The paper ends with a summary of the main findings and an outline of the next phases of the work.

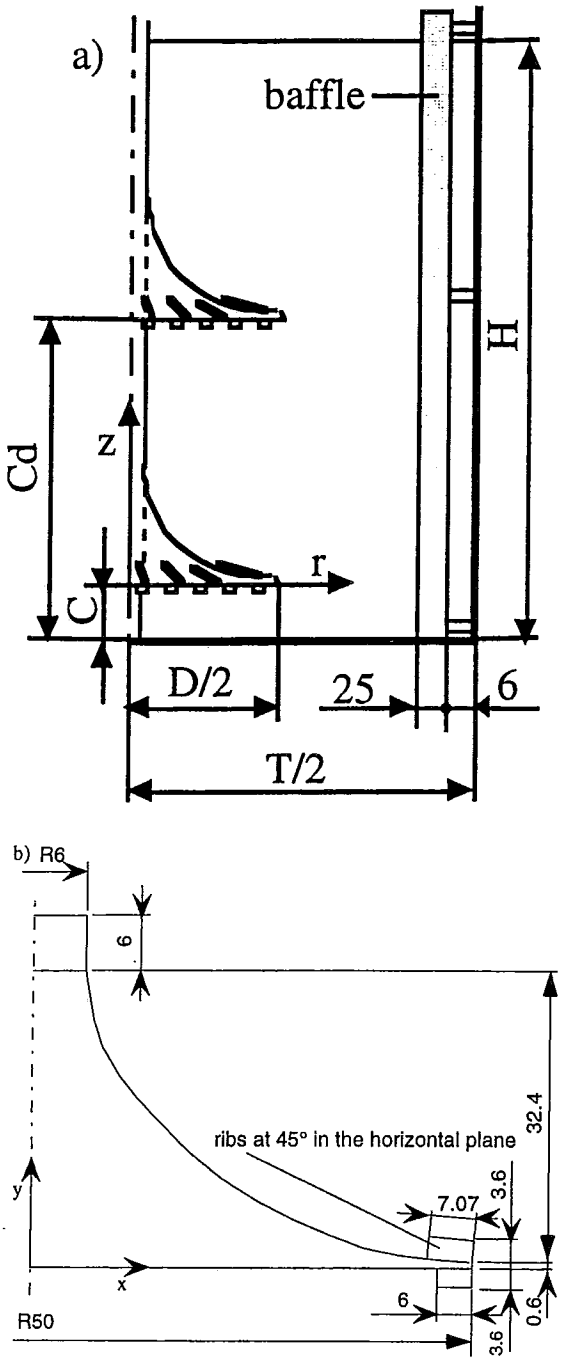

Figure 1 — Geometric characteristics of the stirred vessel and coordinate system (a), and of the 100 mm hyperboloid impeller (b).

Experimental Setup

Stirred vessel

The experimental rig consisted of a 292 mm diameter stirred vessel in acrylic, which was mounted on a support standing directly on a 3-D milling table. The vessel allowed a maximum height of liquid of 600 mm and was mounted inside a square trough filled with the same liquid as the vessel, in order to reduce optical refractions and help maintain a constant temperature in the bath. Four 25 mm wide and 4 mm thick baffles were mounted at 90° intervals within the tank, to avoid solid-body rotation of the fluid. They were attached to small triangular connectors which separated them by 6 mm from the vessel wall, thus eliminating the dead zones normally found behind the baffles. The bottom of the tank was flat and had a bearing embedded in it, to support the drive shaft. Figure 1-a) schematically shows the geometry of the vessel for the double stack configuration. In the single-stack arrangement the upper impeller is removed.

The various impellers tested in both the single and double stack configurations were supplied by Invent GmbH, according to their pattented design. Three hyperboloid impellers had diameters of 70, 100 and 170 mm, respectively, each with 8 transport ribs on their upper surface, but a different number of shear ribs on their bottom surface. The ribs were small rectangles welded to the impeller surface at equally spaced intervals, along their longer dimension, and the number of shear ribs was 48 for the 170 mm impeller and 24 for the 100 and 70 mm impellers. The Rushton

TABLE 1
Coordinates of the 100 mm Diameter Impeller Surface in (mm)

x	6	6	7	8	10	12	14	16	18	20	22	26	30	34	38	42	46	50
y	38.4	32.4	27	24.2	21	18.5	16.5	14.5	12.7	11.1	9.6	7.2	5.3	3.6	2.2	1.4	1.0	0.6

TABLE 2
Dimensions of the Impeller Ribs in (mm)

	170 mm impeller	100 mm impeller	70 mm impeller
Transport ribs (upper)	16.7 × 4.5	10 × 3.6	7.0 × 3.5
Shear ribs (bottom)	6.7 × 3.6	5 × 3.6	4.3 × 3.3

TABLE 3
Main Characteristics of the Laser-Doppler Anemometer in Air at e^{-2} Intensity

Laser wavelength	514.5 nm
Measured half angle of beams in air	3.65°
Dimensions of measuring volume in air	
major axis	2.53 mm
minor axis	162 μm
Fringe spacing	4.041 μm
Frequency shift	0.6 MHz

impeller used in the comparisons had a diameter of 100 mm. The transport ribs and the shear ribs were vertical, at an angle of 45° and 0° relative to a diametral plane, respectively. A general drawing of the hyperboloid agitator is plotted in Figure 1-b), and the coordinates of some of its surface points listed in Table 1. The size of the ribs were not scaled and consequently they are presented in Table 2. More details on the construction of the impeller and ribs can be found in Höfken and Bischof (1993).

The impellers were painted mat black to reduce reflections during the flow visualization and velocity measurements with the Laser-Doppler anemometer. In the single stack configuration the hyperboloid stirrer was positioned with an off-bottom clearance to vessel diameter ratio of 1.3/30, whereas the Rushton impeller was mounted at the standard configuration of 1/3 off-bottom clearance (C/H). In the double stack configuration the second hyperboloid stirrer was mounted one vessel diameter above the lower impeller, defining a clearance ratio of 31.3/30 (C_d/H).

MEASURING EQUIPMENT

On top of the structure standed a 600 W DC servomotor controlled by a variable power supply unit, and the velocity could be monitored on a proper display. A tachogenerator gave an electrical impulse proportional to the speed and controlled it together with an amplifier. An analog output of 0 to 10 V, corresponding to 0 to 3000 rpm was available and as a result, the speed could be kept constant with an uncertainty of around ± 1 rpm, which corresponded to less than 0.5% of the rotational speed. The rotational speed never exceeded 550 rpm to avoid damage of the baffles.

The output of a T4A/50 torquemeter from HBM, consisting of a strain gauge bridge fixed to the surface of the drive shaft between the motor and the stirrer, together with the measurement of the rotational speed, allowed the calculation of the power by a purpose-built electronic multiplying module from HBM, model MGC, after signal amplification was performed. The range of operation of the torquemeter was between 0 and 10 Nm to 50 Nm and the accuracy of each reading was about 10^{-2} Nm.

The measured torque included the torque transmitted to the fluid and the torque loss absorved in all the mechanical contacts. The torque loss was subtracted from the total measured torque to yield the net torque, after measurements were carried out with an empty tank under the same operating conditions that were investigated with the full tank. The uncertainty of the torque measurements varied between 2 and 10% for the higher and lower rotational speeds, respectively, but only the readings having uncertainties of less than 5% were kept and are presented here. More details of the uncertainty analysis of the torquemeter can be found in Piqueiro et al. (1995).

The output from the speed and torque transducers were connected to a computer via an interface A/D card and the statistical quantities were calculated with a special software from samples of at least 200 values and at most a few hundred values, at a data rate of 1.667 Hz.

LASER-DOPPLER ANEMOMETER

A one component Laser-Doppler anemometer from Dantec was used in the forward and back scatter modes for measuring the three components of the mean velocity flow field in one of the tested configurations. The beam from the 100 mW Ar-ion laser, operating in multimode, passed through a series of optical elements before the Bragg cell, where a frequency shift of 0.6 MHz was imposed. To improve the alignement of the optics and reduce the size of the control volume, a pinhole section and beam expander, with an expansion factor of 1.95, were put before the 600 mm front lens. The refraction of the laser beams in the plane and curved walls was calculated and taken into account to correct the positioning of the control volume. Table 3 lists the main characteristics of the Laser-Doppler system.

The scattered light from titanium dioxide 0.22 μm mean diameter seeding particles, supplied by TSI Inc., was collected by the photomultiplier before which stood an interference filter of 514.5 nm. The signal from the photomultiplier was band-pass filtered and processed by a TSI 1990C counter operating in the single measurement per burst mode, with a frequency validation setting of 1% at 10/16 cycle comparison. A 1400 Dostek card interfaced the counter with a 80486 based computer, which provided all the statistical quantities, via a purpose-built software.

Close to the impeller the flow was found to be angle-dependent, as shown by Piqueiro et al. (1996), but in this paper only the overall mean flow pattern is of concern and 360° ensemble-averaged values, calculated from the angle-resolved measurements, are reported. The sample size was 30,000 for data taken far from the impeller, in regions where the flow was not periodic, and of 600,000 realizations close to it. This large sample was necessary to have accurate 1° angle-resolved measurements, from an average 1° sample of

TABLE 4
Fluids and Their Properties at 20°C. Concentrations are by Weight

Fluid	Density [kg/m^3]	Dynamic viscosity [Pa·s]	Refractive index
Pure water	1000	0.001015	1.333
40% glycerin in water	1080	0.004778	–
70% glycerin in water	1140	0.0117	1.4500 (21°C)
Pure glycerin	1200	0.669	1.4726 (21°C)

1,666 readings. The mean velocity uncertainty was assessed to be less than 1.2% at a 95% uncertainty level, assuming a 100% turbulence intensity and following the error analysis procedures outlined in Durst et al. (1981).

The positional uncertainty of the measuring volume was limited by the control volume size, the resolution of the traversing table and the visual method used to locate the control volume in the vessel, and was estimated to be equal to ± 200 μm and ± 140 μm in the horizontal and vertical directions, respectively.

FLUID CHARACTERISTICS

In order to cover as broad a range of Reynolds number as possible, five different Newtonian fluids were used: they ranged from pure water to pure glycerin and some of their properties are presented in Table 4. The temperature of the fluid within the vessel was always carefully monitored for proper data processing.

The density of the fluids was measured with a picnometer and a refractometer Abbe Type 1T was used for the refractive index measurements. The Physica MC100 rheometer with the concentric cylinder Z1-DIN geometry, as described by Pereira and Pinho (1994), was used for the viscosity measurements of the various Newtonian solutions at different temperatures. For the 10 to 30°C temperature range, mathematical functions were fitted to the viscosity data by a least-squares method and the results are presented in Piqueiro (1997).

Results and discussion

The results of the power measurements will be discussed first, and are followed by the description of the mean velocity field. Some of the arguments put forward to explain the results of the power measurements are based on the velocity measurements and on flow visualisation results presented elsewhere (Kunte et al., 1994).

POWER MEASUREMENTS

The power consumption in a stirred vessel depends of the various geometrical parameters shown in figure 1, the rotational speed and the fluid properties. From dimensional analysis arguments this relationship can be put into a compact form:

$$Ne = f\left(Re, \frac{D}{T}, \frac{C}{T}, \frac{H}{T}, \text{impeller}\right) \quad \ldots\ldots\ldots\ldots\ldots (1a)$$

$$Ne = f\left(Re, \frac{D}{T}, \frac{C}{T}, \frac{H}{T}, \frac{C_d}{T}, \text{impeller}\right) \quad \ldots\ldots\ldots\ldots (1b)$$

for the single and double stack configurations, respectively. The acceleration of gravity plays a role whenever surface effects are relevant, but the presence of the baffles destroys the large rotating surface vortex and eliminates the influence of the resulting Froude number.

The Newton and Reynolds numbers in stirred vessel flows are traditionally defined as:

$$Ne = \frac{P}{\rho N^3 D^5} \quad \ldots\ldots\ldots\ldots\ldots\ldots\ldots\ldots\ldots\ldots (2)$$

$$Re = \frac{\rho N D^2}{\mu} \quad \ldots\ldots\ldots\ldots\ldots\ldots\ldots\ldots\ldots\ldots (3)$$

Power measurements were carried out with the three different hyperboloid impellers presented above and with the 100 mm Rushton impeller for comparison purposes. For each hyperboloid stirrer the single and double stack configurations and the fluid height effect were investigated.

The results of Figures 2 to 5 pertain to single impellers and show the influence of fluid height upon the power consumption for both the D/T= 1/3 hyperboloid and Rushton impellers. The ratio of fluid height to vessel diameter (H/T) varied between 1 and 2, and in all cases the power number is a decreasing function at low Reynolds numbers and assumes a constant value at high Reynolds numbers. The inverse law behaviour at low Reynolds numbers is typical of flows dominated by viscous effects, whereas the constant Newton number indicates an inertia-dominated effect, as the power is proportional to the square of the velocity.

The transition between those two asymptotic behaviours is not so smooth with the Rushton impeller as with the hyperboloid stirrer, because of the sharper geometry and ensuing more complex flow structure of the former. The smoother geometric shape of the hyperboloid stirrer delays transition to higher Reynolds numbers ($Re_{tr.} \approx 200$) in comparison to the Rushton turbine ($Re_{tr.} \approx 20$), where the sharp edges of the blades favours an earlier transition into turbulence of the separated flow region behind the blades. The flow visualisation experiments confirmed that at low Reynolds numbers the flow remained attached to the surface of the hyperboloid stirrer. With the Rushton impeller, as the Reynolds number is decreased the form drag contribution to the total drag is reduced, so that its Newton number becomes 50% smaller than the corresponding Newton number for the hyperboloid impeller at the lowest measured Reynolds number.

On the other side, in the high Reynolds number turbulent flow regime the power of the Rushton impeller is more than five times higher than that of the hyperboloid impeller. There is an increase in the power consumption from about 2.5 at a Reynolds number of 200 to 5 at a Reynolds number of 100,000 for the former case. This slow increase of the Newton number within the transitional flow regime is due to the strong contribution to the drag of the separated flow behind the blades and the complex variations of its flow structure documented by Popiolek et al (1987) and Hockey (1990). Both authors have shown that the flow in the vicinity of the Rushton impeller is strongly three-dimensional with separation at the blade edges and a vortex coming out of its backward surface. The whole flow around the blade starts by being laminar, and then the free shear layer downstream of the blade edge becomes turbulent above a critical Reynolds number. As the Reynolds number is further increased this

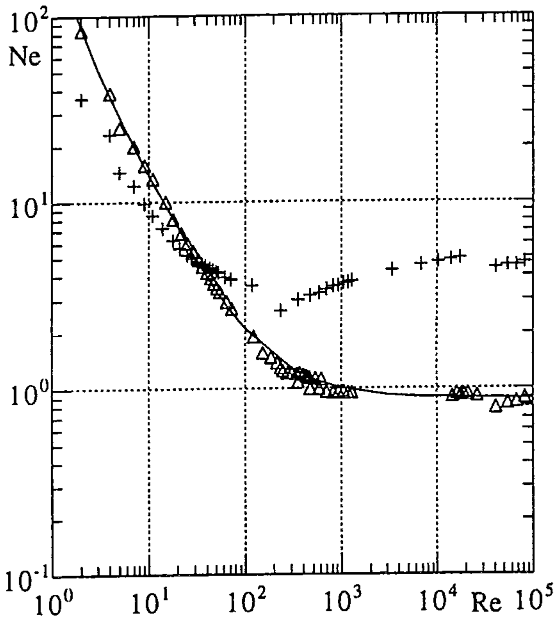

Figure 2 — Newton number versus Reynolds number for the hyperboloid (Δ) and Rushton (+) impellers in the single stack configuration for $H/T = 1$ and $D/T = 1/3$.

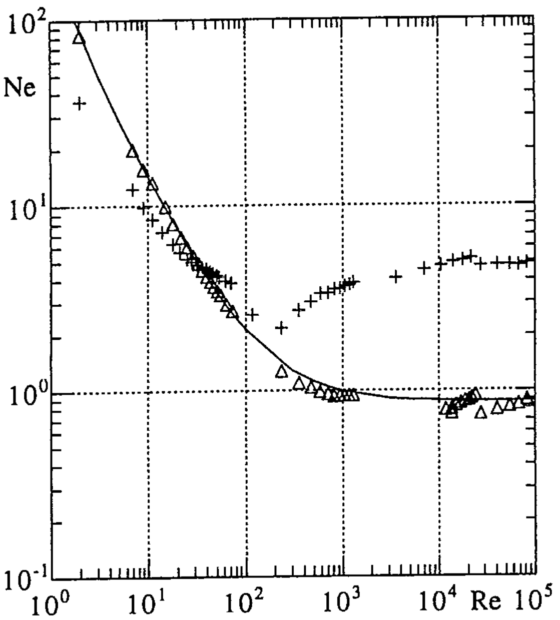

Figure 3 — Newton number versus Reynolds number for the hyperboloid (Δ) and Rushton (+) impellers in the single stack configuration for $H/T = 4/3$ and $D/T = 1/3$.

transitional point moves upstream until the whole separated flow is turbulent although the flow remains laminar in front of the blade. At higher Reynolds numbers the flow in front of the blade also becomes turbulent.

For the hyperboloid impeller, at intermediate transitional Reynolds numbers the Newton number just levels smoothly to a value of about 0.9, suggesting that the flow over the impeller remains attached and turns to turbulent everywhere. This is confirmed by the flow visualisation, by the mean velocity measurements reported in the next section and by the measurements of Nouri and Whitelaw (1994) with a similar impeller having a larger clearance. Note also that, according to Höfken et al. (1991), the hyperboloid

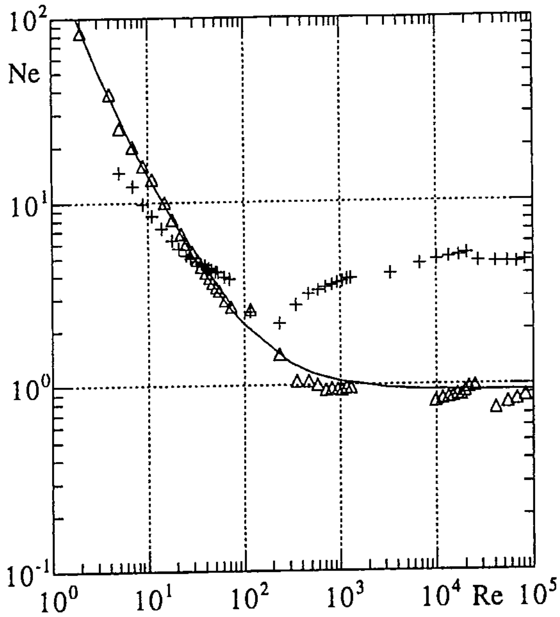

Figure 4 — Newton number versus Reynolds number for the hyperboloid (Δ) and Rushton (+) impellers in the single stack configuration for $H/T = 5/3$ and $D/T = 1/3$.

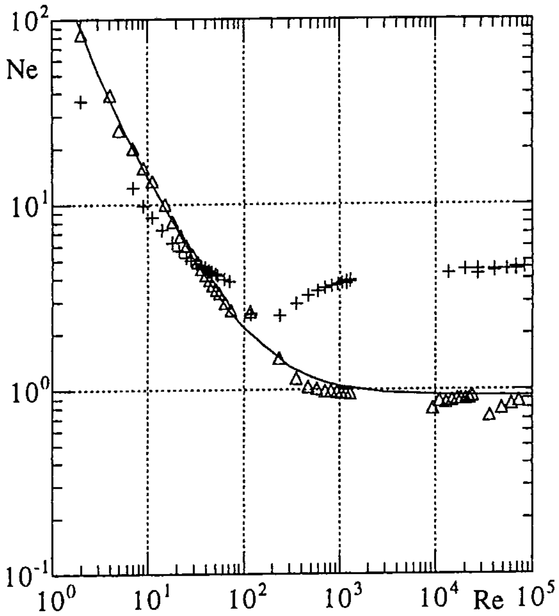

Figure 5 — Newton number versus Reynolds number for the hyperboloid (Δ) and Rushton (+) impellers in the single stack configuration for $H/T = 2$ and $D/T = 1/3$.

impeller was designed from the potential theory equations imposing requirements of a continuously attached flow.

A simplified theoretical analysis of the power consumption drawn by the hyperboloid stirrer can be carried out assuming a purely circumferential, laminar Couette flow at each horizontal plane. For an impeller without ribs and an unbaffled vessel, that yields the following Newton number:

$$Ne = \frac{A}{Re} \quad \text{.............................} \quad (5)$$

where A is a constant. Similarly, for a turbulent flow the calculated power consumption becomes independent of the viscosity and directly proportional to the inertia.

TABLE 5
Power Consumption Correlations with the $D/T = 1/3$ Single Hyperboloid Stirrer as a Function of the Fluid Height (H/T)

$H/T = 1 \Rightarrow Ne = 0.882 + \frac{121.5}{Re} + \frac{87.1}{Re^2}$ (7a)

$H/T = 4/3 \Rightarrow Ne = 0.868 + \frac{126.0}{Re} + \frac{78.0}{Re^2}$ (7b)

$H/T = 5/3 \Rightarrow Ne = 0.926 + \frac{121.1}{Re} + \frac{87.9}{Re^2}$ (7c)

$H/T = 2 \Rightarrow Ne = 0.904 + \frac{121.0}{Re} + \frac{88.0}{Re^2}$ (7d)

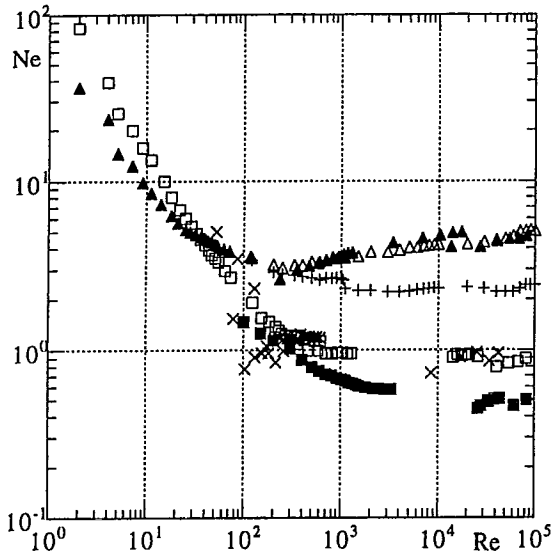

Figure 6 — Newton number versus Reynolds number for $H/T = 1$. Comparison with the literature. This work: × $D/T = 0.24$; □ $D/T = 1/3$, ■ $D/T = 0.58$ Hyperboloid and ▲ $D/T = 1/3$ Rushton. From Hockey (1990): Δ Rushton and + pitched blade.

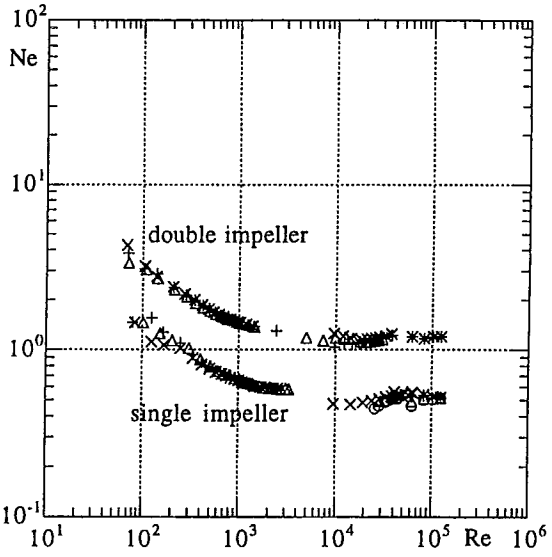

Figure 7 — Newton number versus Reynolds number for the single and double hyperboloid stack shaft. Impeller diameter = 170 mm ($D/T = 0.58$); ○ $H/T = 1$; Δ $H/T = 4/3$; + $H/T = 5/3$; × $H/T = 2$.

The real flow is three-dimensional with axial and radial velocities plus the added effects of the transport and shear ribs and the baffles. Still, the theoretical asymptotic behaviours at low and high Reynolds numbers are qualitatively the same, and it seems appropriate to fit the experimental data with an equation of the type:

$$Ne = \frac{A}{Re} + B + \frac{C}{Re^2} \quad \ldots\ldots\ldots\ldots\ldots\ldots\ldots\ldots (6)$$

where the last term on the right-hand-side corrects for intermediate Reynolds number behaviour.

Equation (6) was least-square fitted to the measured data pertaining to the single hyperboloid impeller of 100 mm of diameter and the outcome is listed in Table 5 and shown in the full lines of Figures 2 to 5. The agreement is good in the laminar regime, but small differences are observed at intermediate and high Reynolds numbers. These differences are due to a lack of well distributed data for Reynolds numbers higher than 100, to the higher experimental uncertainty in some scattered values, associated with low torque measurements in the high Reynolds number region, and finally to the possible need of other corrective terms to account for transitional behaviour. There was a lack of data at high and low Reynolds numbers for the 70 and 170 mm diameter stirrers, thus preventing the fitting of Equation (6) to these cases.

The curves and the data in Figures 2 to 5 show no noticeable effect of the fluid height upon the power consumption for H/T between 1 and 2. This is also found in the parameters of the fitted equations: parameter B has a maximum variation of less than 3.5% around its mean value, and the inverse law parameter A varies slightly less than that. The corrective term shows a higher variation of up to 10%, but at Reynolds numbers of the order of 1, where C/Re^2 starts to be relevant, the lower value of parameter C is always offset by the higher value of A, so that $A/Re + C/Re^2$ is rather constant for the three stirrers.

The effect of the impeller diameter was investigated with three different sizes of the hyperboloid stirrer of 70, 100 and 170 mm, corresponding to impeller to vessel diameter ratios of 0.24, 1/3 and 0.58, respectively. A comparison between the Newton numbers of these three impellers for the H/T=1 configuration is presented in Figure 6 and the scatter of the data pertaining to the smaller impeller (70 mm) is again due to difficulties in measuring very low torque. For the larger impeller the power curve is again smooth and there is a delayed transition from laminar to fully developed turbulent flow relative to the 100 mm impeller. The turbulent flow Newton number is now about 0.5, lower than that of the 100 mm impeller which is equal to 0.9, and for the smaller 70 mm impeller 0.95 was measured. So, an increase in impeller diameter shifts transition from the inverse power law to higher Reynolds numbers and reduces the value of the constant Newton number pertaining to fully developed turbulent flow.

With the 100 mm hyperboloid impeller, the flow at the highest rotational speeds (550 rpm) was rather violent and some air was being entrained from the surface, whereas with the 70 mm diameter impeller the flow visualisation still showed large regions of very slow motion far from the impeller. The flow visualisation also showed that regardless

of the impeller diameter the flow tended to be very weak for fluid levels higher than $H/T = 1$, thus the absence of an effect of the fluid height upon the power consumption, even for the larger impeller (Figure 7). This can be advantageous in applications where air entrainment from the surface is to be avoided. These results also imply the need for a second impeller on the shaft in order to agitate well the fluid in vessels with large fluid heights.

The present results with the Rushton impeller compare well with those of other researchers, such as Nouri (1988) and Nouri and Whitelaw (1990), who reported a Newton number of 5.0 at high Reynolds number flows. In Figure 6 the present measurements with the hyperboloid impellers and the Rushton turbine are compared with data pertaining to the Rushton and the six 45° pitched blade impellers from Hockey (1990), at the same flow configuration. The two sets of experiments differ in the baffle location: in Hockey's work the baffles were directly attached to the vessel wall, whereas in the present case there was a small gap between them and the wall. The collapse of the two sets of Rushton data at intermediate and high Reynolds numbers shows that the influence of the baffle location is minimal. The graph also shows that at identical Reynolds numbers the power consumption of the hyperboloid stirrer is lower than that of the six pitched blade impeller, an agitator which creates a more similar flow pattern and has a power number of 2.2.

There are other low power consumption impellers used in industry and it is important to compare the performance of the hyperboloid stirrer with them. Two of them are the Chemineer and Prochem hydrofoils, which were investigated in some detail by Jaworski et al. (1996). As far as the power consumption is concerned the hyperboloid stirrer performs worse than the Chemineer hydrofoil, but better than the remaining devices (Table 6). It is our belief that the small differences in D/T ratio will not be enough to change this order of performances. Other bulk flow coefficients are also relevant for assessing the relative performance of the stirrers, and in those the hyperboloid stirrer looses some of the advantage, as will be shown in the next section.

Figure 7 compares the performance of the hyperboloid stirrer in the double and single-stack configurations with the larger impeller and also assesses the fluid height effect. In the double-stack configuration, the second impeller was located one vessel diameter above the lower one. There is again no influence of the fluid height upon the normalised power consumption, regardless of the number of impellers, and for the double-stack configuration the Newton number is twice that measured for the single impeller at identical Reynolds number.

The lower impeller being very close to the bottom of the vessel, one could argue that a significant portion of the inputed power would be dissipated between its bottom and the base of the vessel. This geometrical limitation is not present for the upper impeller and yet the power consumption for the double-stack configuration is twice that of a single impeller, thus suggesting that the main contribution to dissipation under the lower impeller can not be attributed to the high shear rates encountered near the bottom wall, but is due to the shear ribs exclusively and that any interference between the two agitators is minimal.

In their measurements with the hyperboloid stirrer at high Reynolds numbers Nouri and Whitelaw (1994) found the Newton number to be equal to 0.178, whereas here it was equal to 0.9. With the clearance effect shown to be irrelevant,

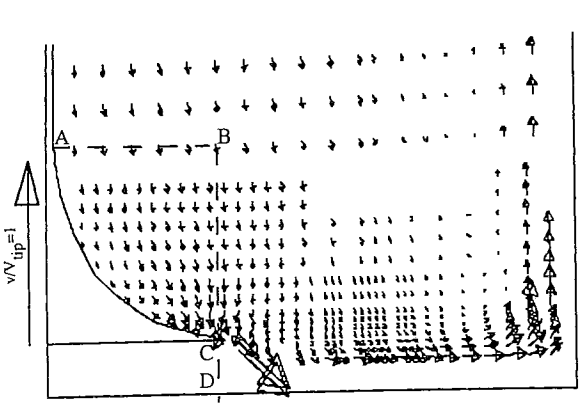

Figure 8 — Vector plot of the mean axial and radial velocity components in a diametral vertical plane in the vicinity of the bottom of the vessel and impeller.

this major difference can only be justified by the fact that their impeller had only 8 transport ribs on the upper surface of the stirrer, whereas here there was an extra set of 24 shear ribs at the bottom surface. The mean flow field measurements to be reported next also confirm that the ribs are responsible for high velocities and shear rates very close to the edge of the impeller and, mostly important, the velocity measurements of Piqueiro et al. (1996) show a strong flow periodicity with much higher velocities and reversed flow near the tip of the impeller, in the region close to the edge of the transport ribs. The reversed flow is not immediately at the impeller surface, but above the very thin strong boundary layer that flows down along it. The lower velocities encountered near the impeller tip, but below the impeller base plane will probably be associated with a high degree of turbulence and flow separation also in the shear ribs. So, it seems that it is the form drag associated with the shear ribs and the increased turbulence under the impeller that are responsible for an increased power need.

The role of the shear ribs is also emphasized by the finding of Nouri and Whitelaw (1994) that the effect of the impeller diameter upon the Newton number was opposite to that reported here. With a negligible clearance effect, that difference must again be attributed to the role of the shear ribs and to the fact that dimensional similarity was not respected here between the different impellers, regarding rib size and number. The smaller impeller had relatively larger and fewer ribs, especially shear ribs, than the larger impellers (Table 2).

Mean flow field

The mean flow field was investigated in two different ways: for a qualitative inspection of the flow with both the single and the double stack impeller configurations, the flow was seeded with aluminium powder and a cylindrical lens was used to create a plane of laser light to iluminate the flow using a 5W Ar-ion laser. The detailed description of these experiments and their results are presented in Kunte et al. (1994) and only some of them will be reminded here. A more detailed quantitative flow description involving velocity measurements by Laser-Doppler anemometry was then performed for a high Reynolds number flow (Re = 50,000) with the 100 mm hyperboloid impeller.

The flow visualisation was difficult to perform because the flow is strongly three-dimensional, with small velocities in all three-directions, except close to the impeller where

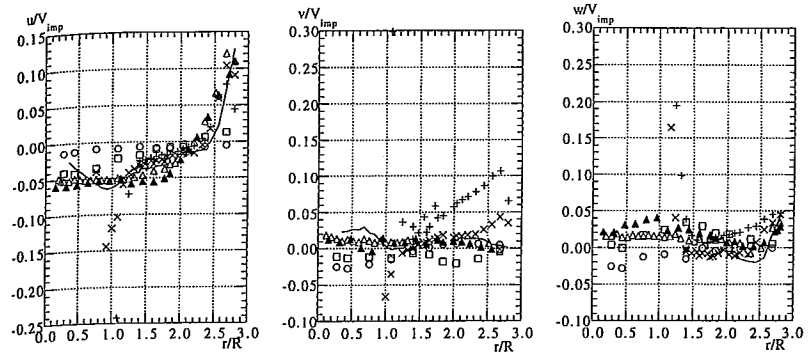

Figure 9 — Radial profiles of the mean axial (u), radial (v) and tangential (w) velocities at typical horizontal planes. + z = –3; × z = +3; — z = +15; Δ z = +40; ▲ z = +90; □ z = +190; ○ z = +270.

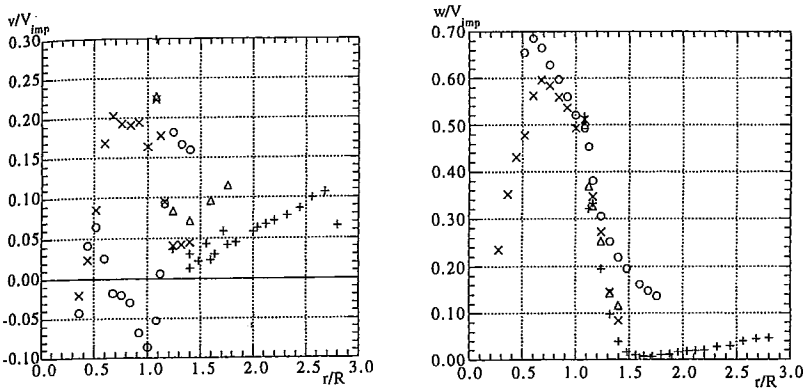

Figure 10 — Radial profiles of the mean radial (v) and tangential (w) velocities below the impeller. ○ z = –10; x z = –6; Δ z = –5; + z = –3.

there is a predominance of one or two velocity components. The overall flow was found to be similar to the pattern described by Nouri and Whitelaw (1994) for their lower clearance case; the flow remained attached to the upper impeller surface regardless of the Reynolds number, which affected only the flow away from the impeller.

This impeller has mixed characteristics in that, although it operates at high rotational speeds as Rushton or pitched blade impellers do, there is neither a very strong primary tangential flow nor an intense secondary radial flow in the bulk of the vessel; such high velocities are encountered exclusively in the near vicinity of the impeller surface, as is clear from the mean velocity measurements.

For the double-stack configuration the flow above both impellers was seen to be identical and there was no effect of the upper impeller upon the flow in the lower impeller. Below the lower agitator the main flow was tangential especially near the bottom of the vessel (see also Fig. 10) and it was superimposed on a weak outwards radial flow close to the impeller periphery and an inwards radial flow at the bottom wall of the vessel, thus forming an irregular and weak ring vortex in the vertical radial plane, as was also observed in the single impeller case. Below the upper impeller, the absence of a wall directly beneath the stirrer did not create this small vortex, rather a large one, but the velocities were small. Here, the induced tangential flow was superimposed on a radial outwards flow close to the edge of the impeller, and there was a very weak axial flow coming upwards from below, along the shaft. There seemed to be no major influence of the flow generated by the lower impeller upon the flow around the upper one, beyond these small differences due to the absence of the base wall.

For the single impeller case, the Reynolds number increase raised the turbulence and caused the flow going up along the vessel walls to roll up, detach and go into the bulk flow that goes down towards the impeller, thus defining a large vortex ring in the vertical plane. Both the flow visualisation and the velocity measurements confirmed that the flow always remained attached to the impeller surface, and the small region of reversed flow near the tip of the impeller surface could only be measured during the angle-resolved velocity measurements and occurred at the edge of the boundary-layer (Piqueiro et al., 1996). The main mean flow pattern is illustrated in the vector plot of the mean axial and radial velocity components in Figure 8.

The figure shows a predominantly downward axial flow, with an average magnitude of about 5% of the impeller tip velocity over 70% of the radius of the vessel. Then, mass conservation requires a stronger upwards axial flow close to the vessel side wall, reaching a maximum of 15% of the impeller tip velocity. Near the tip of the impeller, the long vectors show that the velocities are very intense because the flow is being pushed directly by the eight transport ribs. So, the boundary-layer over the impeller surface is accelerated and becomes very thin as it leaves the tip of the impeller.

The various radial profiles of the three components of the velocity vector shown in Figures 9 and 10 complete this description. A strong radial velocity component is acquired by the fluid only very close to the impeller surface, and especially at the bottom of the vessel (z = –3 and +3 mm). On the upper half of the vessel (z > +140 mm) the fluid moves slowly towards the shaft, with a magnitude of about 2% of the tip velocity, whereas the outwards radial flow between z = +20 to z = +90 mm is also of about 2% of the tip velocity (the impeller is 40 mm high). Closer to the bottom, in a region also influenced by the agitator, the radial velocities are higher than above because the fluid is being pushed by the shear ribs, reaching maximum values of about 10% of the tip velocity away from the impeller and of about 20 to 30% very close to and under the impeller. The large vortex defined by the circulating flow pattern around the vessel is centered at around r/R = 2.4 and z/R = 1.75 and close to the

TABLE 6
Power Number and Flow Discharge Coefficients at High Reynolds Number Flows

Stirrer	D/T	Ne	Fl_c	Fl	E_2	E_c
Rushton	1/3	5.0	2.10	0.74	1.85	0.023
Hyperboloid	1/3	0.9	0.57	0.13+ (> 0.26)	0.2	0.0025
Chemineer [*]	0.46	0.305	0.74	0.41	1.32	0.059
Prochem [*]	0.35	1.58	1.55	0.82	2.35	0.036
Six 60° pitched blade [**]	1/3	2.2		0.94		

+ refers to the upper control volume defined by the dashed ABC line, only.
* from Jaworski et al. (1996).
** from Hockey (1990).

free surface ($z > +190$ mm), but especially above $z = +240$ mm, the measured axial and radial velocity components tend to zero, i.e., the fluid is almost motionless.

The magnitude of the mean tangential velocity component is similar to that of the radial velocity, except near the impeller and the ribs. Far from the agitator the fluid rotates slowly in the same direction as the impeller, with velocities between 1 to 4% of the impeller tip speed. Below the impeller base plane the tangential velocities are very high because of the presence of the shear ribs, reaching 70% of the tip velocity under the impeller but decreasing very quickly with the radius, dropping from over 40% of the tip velocity at $r/R = 1.08$ to less than 10% at $r/R = 1.4$.

Below the impeller the rotation of the fluid is always positive, but not above its base plane ($z = +3$). From a radial position of about $r/R = 1.5$ and up to the vessel side wall the fluid rotates in the opposite direction to the impeller, with the higher negative velocity of around 2.5% of the tip velocity occurring close to the wall. This counter-rotating flow disappears for heights 60 mm above the impeller base plane, and could be due to the simultaneous influence of the baffles and a low pressure created by the high speed jet at the bottom wall.

The velocity measurements allowed the calculation of some bulk flow parameters useful for assessing the strength of the flow within the vessel (Oldshue, 1983). The positive and negative axial velocities induced by the impeller were integrated at various horizontal planes to quantify positive and negative flow rates (Q^+ and Q^-) according to:

$$Q^+ = 2\pi \int_{r_{(u=0)}}^{r_{wall}} r u_z(r) dr$$

$$Q^- = 2\pi \int_{r_{shaft}}^{r_{(u=0)}} r u_z(r) dr \quad \ldots\ldots (8)$$

The maximum value of Q defined the circulation flow rate (Q_c), which was normalised into a circulating flow number (Fl_c) as:

$$Fl_c = \frac{Q_c}{ND^3} \quad \ldots\ldots (9)$$

Another important parameter is the normalised pumping capacity (Fl) which is defined as in equation (9), with the pumping capacity (Q_p) taking the place of Q_c. The pumping capacity is the flow rate passing through the control volume defined by the impeller which, considering the geometry and the way the hyperboloid impeller works, would be zero, were it not for the small control volume associated with the shear and transport ribs. Anyway, it is important to quantify the flow in the close vicinity of the impeller and for that purpose a different control volume was defined instead, represented by the dashed line ABCD in Figure 9. There was not enough detailed data to accurately calculate the flow rate crossing the control volume at CD, below the impeller, so the values reported here concern only the upper control volume ABC.

Q_p could be calculated as a function of either the axial velocity crossing the horizontal plane AB, or the radial velocity crossing surface BC. It was found that accross the surface BC about 90% of the flow rate passed within the 3.6 mm closer to the impeller, i.e., the strong push given by the transport ribs is responsible for the pumping capacity of the hyperboloid impeller. Below the impeller the radial velocities were higher than above and over a larger height, so the contribution to the total pumping capacity should be higher than that of the upper control volume, raising Fl from 0.13 to at least 0.26.

To estimate the circulation efficiency of the impellers the circulation flow number can be related to the corresponding Newton number in various ways that are summarized in Jaworski et al. (1996). The efficiency criteria of equations (10-a) and (10-b) were selected for comparisons among data pertaining to the Rushton, 60° six pitched blade impeller, two hydrofoils investigated by Jaworski et al. (1996) and the 100 mm hyperboloid impeller and the results are listed in Table 6.

$$E_2 = \frac{Fl_c^3}{Ne} \quad \ldots\ldots (10\,a)$$

$$E_c = \frac{Fl_c^3}{Ne}\left(\frac{D}{T}\right)^4 \quad \ldots\ldots (10\,b)$$

The impeller to vessel diameter ratio is not the same for all the agitators but they are fairly similar and the differences are not expected to change the qualitative ordering of the impellers. The data shows that the hyperboloid impeller has a low power consumption, but that is also associated with a slow circulating flow which reduces its efficiency number (E_c) to values about 10 to 20 times lower than that of other impellers. Therefore, as far as these hydrodynamic parameters are concerned, the hyperboloid agitator is rather inneficient and it is now necessary to carry out measurements of the magnitudes of the shear rates and of the micromixing and especially of process engineering quantities in order to make a final judgement of its performance.

In spite of these apparent shortcomings, this low clearance-low power agitator has been successful in operations

of denitrification and maintenance of complete suspension within waste water treatment plants in Germany, in combination with new aeration and process control methodologies which were reported by Höfken and Bischof (1993) and Höfken et al. (1994 a,b). This is due to the high velocities encountered at the bottom of the vessel which are important to ensure solids suspension and a quick spread of gas in aerated systems. Simultaneously, the lower velocites above reduce damage to microorganisms in suspension, thus avoiding the reduction in yield due to destruction of agents that can be found in more violent and well mixed flows (Höfken et al., 1991). Definitely, this calls for further research targeted onto process engineering quantities, especially in this area where the hyperboloid agitator has been more industrially successful.

Conclusions

Flow visualization, mean velocity and power measurements were carried out in a stirred vessel powered by hyperboloid impellers and the results were compared with those pertaining to a Rushton turbine and other data from the literature. The main findings were the following:

– The flow in the vessel powered by a single hyperboloid agitator was a complex three-dimensional flow with predominant velocity components only in the vicinity of the impeller. The flow came down along the shaft onto the upper surface of the impeller, where it remained fully attached, before leaving it radially;

– An increase in the hyperboloid stirrer diameter shifted the transition from the inverse to the constant Newton number laws to higher critical Reynolds numbers; it also reduced the value of the constant Newton number pertaining to high Reynolds number turbulent flow, due to the effect of the ribs which were relatively larger and fewer for the smaller agitator, in violation of geometric similarity. The Newton number at high Reynolds number flows was of 0.5, 0.9 and 0.95 for the 170, 100 amd 70 mm hyperboloid stirrer, respectively;

– For the double stack configuration, the flow induced by any of the impellers had no detectable influence upon the flow in the region dominated by the other agitator and the Newton number was twice the value for a single agitator, at the same Reynolds number. The effect of the clearance upon the power consumption was thus found negligible;

– For H/T between 1 and 2 the fluid height variation did not affect the Newton number, regardless of the size and number of impellers;

– In the standard configuration, the power consumption of the hyperboloid stirrer was twice that of the Rushton impeller under laminar flow conditions, but five times lower at high Reynolds number flows and two and a half times lower than that of a 60° six pitched blade impeller, also in the turbulent regime. The lower power consumption was accompanied by a reduction of the pumping capacity number by more than 550% and 700% relative to the Rushton and pitched blade impellers, respectively. On the basis of these same parameters, the hyperboloid performed worse than other low power agitators;

– The shear ribs were found to be the main responsible for the increased power consumption relative to the non shear ribbed agitator of Nouri and Whitelaw (1994) and it was also found that the close clearance to the bottom of the vessel did not affect sigificantly the power consumption;

– To better assess the performance of the hyperboloid impeller further measurements are required: detailed angle-resolved mean and turbulent velocity measurements will enable to quantify the magnitudes of shear rates and micromixing, and process engineering quantities, such as solid suspension, mixing time and yield with aeration and under more realistic conditions.

Acknowledgements

The authors would like to thank the European Commission and JNICT- Junta Nacional de Investigação Científica, for making possible this work through the contracts number JOU 2- CT9- 0127 and PEAM/C/TAI/265/93, respectively. Special thanks are due to Mr. Stefan Kunte and Mr. Michael Anbergen who helped with some of the measurements and to Mr. Jerónimo de Sousa for his technical support.

Nomenclature

C = impeller off-bottom distance (m)
C_d = separation of impellers for the double stack configuration (m)
D = impeller diameter (m)
E_2 = circulation efficiency for constant D/T impellers, Equation (11-a)
E_c = circulation efficiency for comparing impellers with different D/T, Equation (11-b)
Fl = pumping capacity number, as in Equation (9)
Fl_c = circulation flow number, Equation (9)
H = liquid height (m)
N = rotational speed (rev/s)
Ne = Newton or power number, Equation (2)
Q_c = circulating flow rate, Equation (8), (m^3/s)
Q_p = pumping capacity (m^3/s)
Q_t = tangential flow rate, Equation (10) (m^3/s)
Re = Reynolds number, Equation (3)
t = temperature (°C)
T = tank diameter (m)
u_z = axial velocity component (m/s)

Greek letters

ρ = liquid density (kg/m^3)
μ = liquid dynamic viscosity (Pa·s)

References

Bakker, A. and H. E. A. van den Akker "The use of profiled axial flow impellers in gas–liquid reactors", in "Proc. Fluid Mixing IV", Inst. Chem. Eng. Symp. Series No. 121 (1990), pp. 153–160.

Buckland, B. C., K. Gbewonyo, D. DiMasi, G. Hunt, G. Westerfield and A. W. Nienow "Improved performance in viscous mycelial fermentation by agitator retrofitting" Biotechnol. Bioeng. **31**, 737–742 (1988).

Durst, F., A. Melling and J. H. Whitelaw "Principles and Practice of Laser-Doppler Anemometry" 2nd edition, Academic Press (1981).

Hockey, R. M. Turbulent Newtonian and Non-Newtonian Flows in a Stirred Reactor. PhD Thesis, University of London, London (1990).

Höfken, M., F. Bischof and F. Durst, Novel Hyperboloid Stirring and Aeration System for Biological and Chemical Reactors. ASME FED-Industrial Applications of Fluid Mechanics **132**, 47 (1991).

Höfken, M. and F. Bischof "Hyperboloid stirring and aeration system: operating principles, application, technical description." Invent GmbH report, version 1.1, Erlangen (1993).

Höfken, M., K. Zähringer and F. Bischof, "Stirring and Aeration System for the Upgrading of Small Waste Water Treatment Plants", Wat. Sci. Tech. **29**, 149 (1994 a).

Höfken, M., F. Bischof, K. Zähringer and F. Durst "Submersed Mechanical Aeration System for Activated Sludge Tanks." ASME FED- Aeration Technology, R. E. A. Arndt and A. Prosperetti, Editors **187**, 47 (1994 b).

Jaworski, Z., A. W. Nienow and K. N. Dyster "An LDA Study of the Turbulent Flow Field in a Baffled Vessel Agitated by an Axial, Down- Pumping Hydrofoil Impeller" Can. J. Chem. Eng. **74**, 3–15 (1996).

Joosten, G. E. H., J. G. M. Schilder, and A. M. Broere "The Suspension of Floating Solids in Stirred Vessels" Trans. J. Chem. Eng. **55**, 220 (1977).

Kunte, S., M. Höfken and T. Valente "The design, Construction, Assembly and Test of an Experimental Facility for Mixing Experiments" Joule project CT 92-0127 report, Lehrstuhl für Strömungsmechanik, Universität Erlangen- Nürnberg, FRG and Laboratório de Hidráulica, Recursos Hídricos e Ambiente, Faculdade de Engenharia da Universidade do Porto, Portugal (1994).

Kusters, K. A. "The Influence of Turbulence on Aggregation of Small Particles in Agitated Vessels" PhD Thesis. Technical University of Eindhoven (1991).

Nagata, S. "Mixing: Principles and Applications" John Wiley & Sons., New York (1975).

Nouri, J. M. "Single and Two-Phase Flows in Ducts and Stirred Reactors" PhD Thesis. University of London, London (1988).

Nouri, J. M. and J. H. Whitelaw "Effect of Size and Confinement on the Flow Characteristics in Stirred Reactors" in Proc. 5th Int. Symp. on Applications of Laser Techniques to Fluid Mechanics, paper 23.2, Lisbon, Portugal, 9–12 July (1990).

Nouri, J. M. and J. H. Whitelaw "Particle Velocity Characteristics of Dilute to Moderately Dense Suspension Flows in Stirred Reactors", Int. J. Multiphase Flow **18**, 21 (1992).

Nouri, J. M. and J. H. Whitelaw "Flow Characteristics of Hyperboloid Stirrers" Can. J. Chem. Eng. **72**, 782 (1994).

Oldshue, J. Y. "Fluid Mixing Technology", McGraw-Hill, New York (1983).

Pereira, A. S. and F. T. Pinho "Turbulent Pipe Flow Characteristics of Low Molecular Weight Polymer Solutions. J. Non-Newt. Fluid Mech. **55**, 321 (1994).

Piqueiro, F. T. "Analysis of the flow field and mixing efficiency of the flow induced by turbine agitators", Department of Civil Engineering, Faculty of Engineering, Porto, Portugal, PhD Thesis in preparation (1997).

Piqueiro, F. M., J. T. Valente, F. T. Pinho "Power consumption and flow pattern of the mixing vessel flow with single and double hyperboloid stirrers" Internal report of the Departments of Civil and Mechanical Engineering, Faculty of Engineering, Porto, Portugal (1995).

Piqueiro, F. M., M. F. Proença, F. T. Pinho and A. M. Santos "Mean and turbulent flow characteristics of single hyperboloid impeller stirred vessels" Proceedings of the Eight International Symposium on Applications of Laser Techniques to Fluid Mechanics, 7–11 July, paper 8.3 (1996).

Popiolek, Z., M. Yianneskis and J. H. Whitelaw "An Experimental Study of Steady and Unsteady Flow Characteristics of Stirred Reactors", J. Fluid Mech. **175**, 537 (1987).

Reed, X. B., M. Princz and S. Hartland "Laser-Doppler Measurement of Turbulence in a Standard Stirred Tank", in Proc. 2nd Euro. Conf. Mixing, Paper B1, Cambridge, UK, March 30–April 1 (1977).

Rutherford, K., S. M. S. Mahmoudi, K. C. Lee and M. Yianneskis "Hydrodynamic characteristics of dual Rushton impeller stirred vessels", AIChEJ **42**, 332 (1996 a).

Rutherford, K., S. M. S. Mahmoudi, K. C. Lee and M. Yianneskis "The influence of Rushton impeller blade and disc thickness on the mixing characteristics of stirred vessels", Trans. Inst. Chem. Eng., **74**, 369 (1996 b).

Skelland, A. H. P. "Non-Newtonian Flow and Heat Transfer", John Wiley & Sons, New York (1967).

Skelland, A. H. P. "Mixing and Agitation of non-Newtonian fluids" in Handbook of Fluids in Motion, (Eds. N. P. Cheremisinoff and R. Gupta), Ann Arbor Science Publishers, Ann Arbor (1983).

Ulbrecht, J. J. and G. K. Patterson (Editors) "Mixing of Liquids by Mechanical Agitation" Chemical Engineering Series: Concepts and Reviews, Volume 1, Gordon and Breach Science Publishers, London (1985).

Manuscript received November 29, 1996; revised manuscript received May 15, 1997; accepted for publication May 29, 1997.